Available online at www.sciencedirect.com

SciVerse ScienceDirect

journal homepage: www.elsevier.com/locate/he

Synthesis and characterization of NiO/GDC–GDC dual nano-composite powders for high-performance methane fueled solid oxide fuel cells

Jae-Ha Myung [a,b], *Hyun-Jun Ko* [a,b], *Jong-Jin Lee* [a], *Ji-Hwan Lee* [a], *Sang-Hoon Hyun* [a,*]

[a] *School of Advanced Materials Science and Engineering, Yonsei University, 134 Shinchon-dong, Seodaemungu, Seoul 120-749, South Korea*
[b] *Specialized Graduate School of Hydrogen & Fuel Cell, Yonsei University, Seoul 120-749, South Korea*

ARTICLE INFO

Article history:
Received 4 April 2012
Received in revised form
25 April 2012
Accepted 30 April 2012
Available online 30 May 2012

Keywords:
Solid oxide fuel cell
Nano-composite powder
Tape-casting
Lamination
Co-firing
Flatness

ABSTRACT

GDC (gadolinium-doped ceria) is well known as a high oxygen ionic conductor and is a catalyst for the electrochemical reaction with methane fuel leading to the oxidation of deposited carbon that can clog the pores of the anode and break the microstructure of the anode. NiO/GDC–GDC dual nano-composite powders were synthesized by the Pechini process, which were used as an AFL (anode functional layer) or anode substrates along with a GDC electrolyte and LSCF–GDC cathode. The anodes, AFL, and electrolyte were fabricated by a tape-casting/lamination/co-firing. NiO–GDC anode and NiO/GDC–GDC anode-supported unit cells were evaluated in terms of their power density and durability. As a result, the NiO/GDC–GDC dual nano-composite demonstrated an improved power density from 0.4 W/cm^2 to 0.56 W/cm^2 with H_2 fuel/air and from 0.3 W/cm^2 to 0.56 W/cm^2 with CH_4 fuel/air at 650 °C. In addition, it could be operated for over 500 h without any degradation with CH_4 fuel.

1. Introduction

Solid oxide fuel cells have been intensely investigated as a next generation green energy system because they have a high efficiency and generate low pollution emissions [1–4]. Moreover, they can use hydrocarbon fuels in an internal reforming reaction or direct electrochemical reaction without an external reforming reactor. However, carbon coking, which degrades the cell performance due to plugging and crashing of the anode microstructure, occurs on the Ni-based anode when a hydrocarbon fuel is used [5–7].

Various research groups have strived to prevent the carbon coking phenomena when directly using hydrocarbon fuel by optimizing the operating conditions including the fuel flow rate and steam to carbon ratio (S/C), and using dopants such as alkali or transition metals including Li, Na, K, Mo, Rh, W, and fluorite structured materials such as LSGM and LSCM [8–13].

The activity of NiO–YSZ anodes is relatively low for intermediate/low temperature SOFCs due to the low ionic conductivity of YSZ at low temperatures. Therefore, NiO–GDC cermets are conventionally used as the anode of SOFCs and have been extensively studied recently. GDC is not only

* *Corresponding author*. Tel.: +82 2 2123 2850; fax: +82 2 365 5882.
E-mail addresses: prohsh@yonsei.ac.kr, cprocess@yonsei.ac.kr (S.-H. Hyun).
0360-3199/$ – see front matter Copyright © 2012, Hydrogen Energy Publications, LLC. Published by Elsevier Ltd. All rights reserved.
doi:10.1016/j.ijhydene.2012.04.140

a higher ionic conductor than YSZ at low temperatures but as the catalyst for the electrochemical reaction, it can prevent carbon coking [14–17].

In this study, NiO/GDC–GDC dual nano-composite powder was synthesized by modifying our previously reported NiO/YSZ–YSZ dual nano-composite powder, which assumed the form of nano-sized NiO and GDC particles (10–20 nm in diameter) homogenously coated on 400 nm sized GDC core particles [18,19].

The unit cells used NiO/GDC–GDC dual nano-composite powder as the anode or AFL, and were subjected to cell performance and durability testing with H_2 and CH_4. Also, the flatness of the 5×5 cm^2 unit cells was optimized by evaluating various loading rates, green tape thicknesses, and the ratio of the anode and electrolyte via tape-casting/lamination/co-firing techniques.

2. Experimental

2.1. Preparation of NiO/GDC–GDC dual nano-composite powder

NiO/GDC–GDC dual nano-composite powders synthesized using the Pechini process as described in our previous work were used as the anode functional layer (AFL) between the porous anode support and the dense electrolyte or as the whole anode support component to improve the cell performance [20,21]. Briefly, the precursors of $Ni(NO_3)_2 \cdot 6H_2O$ (Junsei Chemical Co., 97.0%), $GdN_3O_9 \cdot 6H_2O$ (Aldrich, 99.9%), and $Ce(NO_3)_3 \cdot 6H_2O$ (Kanto Chemical Co., 99.99%) were added to DI water and heated to 40 °C. Next, citric acid (Junsei Chemical Co., 99.5%) and ethylene glycol (Ducksan Pure Chemical, 99.5%) were added to this solution as complexation and polymerization agents, respectively, at 60 °C. Then, GDC powder (Rhodia, ULSA grade) was added to the aqueous solution. The polymeric solution was condensed at 180 °C for 4 h and ash-colored intermediates were obtained. Finally, dual nano-composite NiO/GDC–GDC powders were obtained after calcination at 600 °C for 2 h. The distributions of adhered nano-sized NiO and GDC on the core GDC powder were confirmed by SEM-EDX (JEOL). The degradation of the anodic performances of conventional NiO–GDC and NiO/GDC–GDC anodes were evaluated by measuring the electrical conductivity of the electrodes during thermal cycling. The thermal cycling test was conducted under redox atmosphere. The cycling condition consisted of two steps. The first one was that a specimen was partially oxidized at 650 °C. In order to prevent the catastrophic failure by sudden volume change, the oxidation was performed by exposing the system to an air atmosphere. Heating was from 100 °C to 650 °C with 5 °C/min rate. The other step was the re-reduction of the partially oxidized sample at 650 °C. The electrical conductivity was measured in 3 h after reducing at 650 °C, these steps were repeated for 30 times.

2.2. Fabrication of unit cells via tape-casting/lamination/co-firing

Fig. 1 shows the fabrication procedure of the SOFC unit cells, as reported in our previous investigation [22–24]. As shown in Table 1, ethanol and toluene-based slurries for the NiO–GDC anode/AFL, NiO/GDC–GDC anode/AFL, and GDC electrolyte were prepared using commercial powders of NiO (Nickelous Oxide Green, J.T. Baker, USA), GDC (Rhodia, ULSA grade), carbon black (Raven 430, Columbian Chemical, USA) as a pore former, and EFKA4340 (BASF, Netherlands) as a dispersant. In this study, we also optimized the flatness of the planar-type unit cell because the flatness can seriously affect its performance as a flatter cell can lead to a better contact area for a current collector and a smaller contact resistance as well as reduce the possibility of cell fracturing during cell stacking. The flatness of the unit cell is significantly related to the ratio of the anode/electrolyte thicknesses, the thickness of the anode green sheet, and loading during co-sintering.

Table 2 shows the four types of unit cells used in this study. Cell 1 was laminated and co-fired with a NiO–GDC anode and GDC electrolyte. Cell 2 was laminated with a NiO–GDC anode, mechanically mixed NiO–GDC AFL, and electrolyte. Cell 3 was laminated with a NiO–GDC anode, NiO/GDC–GDC anode functional layer (AFL), and electrolyte. Cell 4 was laminated with a NiO/GDC–GDC anode and electrolyte. Finally, the cathode with a composition of 50 wt% LSCF and 50 wt% GDC

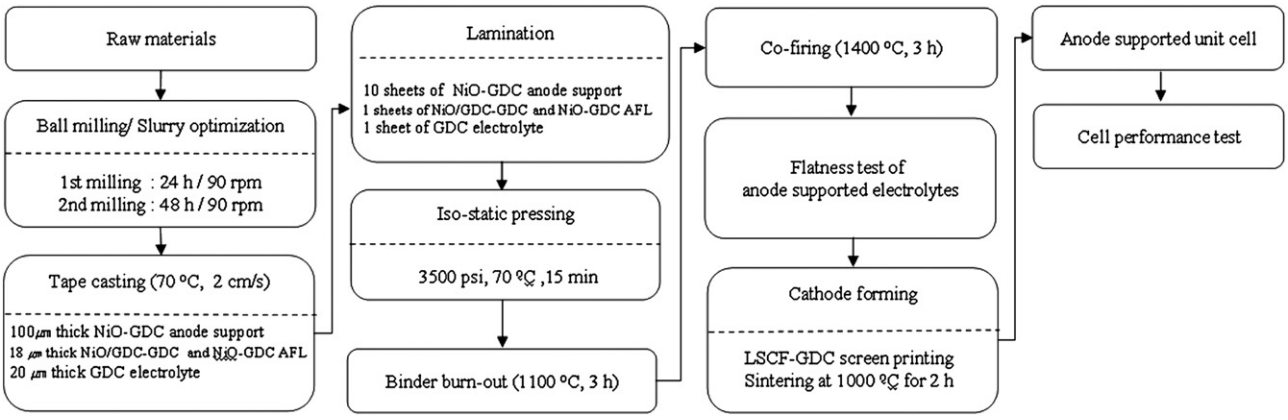

Fig. 1 – Flow chart of the fabrication procedure of the SOFC unit cells.

Table 1 – The compositions of tape-casting: slurries used for the anode, anode functional layer, and electrolyte.

Materials components	Powders (100 g batch)				Solvent (g)		Dispersant (g) (EFKA4340)	Binder solution (g) (B74001, Ferro)
	NiO	GDC	NiO/GDC –GDC	Carbon black	Toluene	EtOH		
NiO–GDC anode	54.94	35.06	–	10	40.25	10.13	2	43
NiO/GDC–GDC anode	–	–	90	10	60.8	15.2	3.48	43
NiO–GDC AFL	61.04	38.96	–	–	60.8	15.2	3.48	43
NiO/GDC–GDC AFL	–	–	100	–	60.8	15.2	3.48	43
GDC electrolyte	–	100	–	–	58	12	0.6	40

Table 2 – The components of the 4 types of unit cells.

Types	NiO–GDC anode	NiO/GDC–GDC anode	NiO–GDC AFL	NiO/GDC–GDC AFL	GDC electrolyte	LSCF–GDC cathode
Cell 1	O	X	X	X	O	O
Cell 2	O	X	O	X	O	O
Cell 3	O	X	X	O	O	O
Cell 4	X	O	X	X	O	O

was screen-printed and fired at 1000 °C after co-firing of the laminate at 1400 °C.

2.3. *Cell performance tests*

The unit cell performance was measured using apparatuses designed and built by our laboratory, as described in our previous report [20]. The performance of the button-type unit cells was analyzed at 650 °C in reactive gases of H_2 (100 cc/min under standard ambient temperature and pressure) or dry methane without any balanced gas (25 cc/min under standard ambient temperature and pressure) at the anode and air (500 cc/min under standard ambient temperature and pressure) at the cathode. In the case of the 5×5 cm^2 planar-type unit cell, the cell performances were evaluated at 650 °C in reactive gases of H_2 (250 cc/min), dry methane (200 cc/min), and air (1200 cc/min) in SUS316L housing. The *I–V* curves and durabilities were measured using a multi-functional electronic load module (3315D, Taiwan). AC impedance measurements were conducted utilizing a Solatron 1260 frequency analyzer and a Solatron 1287 interface.

3. Results and discussion

3.1. *NiO/GDC–GDC dual nano-composite powder*

The NiO/GDC–GDC dual nano-composite powders assumed the form of nano-sized NiO and GDC particles (10–20 nm in diameter) homogenously coated on the 400 nm sized GDC core particles, as shown in Fig. 2.

The microstructural morphology and composition distribution of the composite powders were confirmed by SEM-EDX (JEOL) and X-ray diffraction (Ringaku), as shown in Fig. 3. These well synthesized dual nano-composite powders possess the following excellent properties. The homogeneously distributed and nano-sized NiO on core GDC showed an electrical conductivity of 1500 S/cm, which is higher than the 1250 S/cm obtained from the mechanical mixture of NiO and GDC. It was confirmed that the NiO/GDC–GDC composite anode

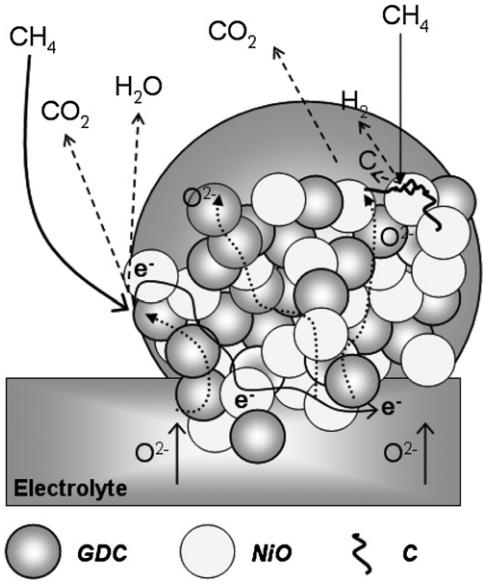

Fig. 2 – Ideal structure of the NiO/GDC–GDC nano-composite powder.

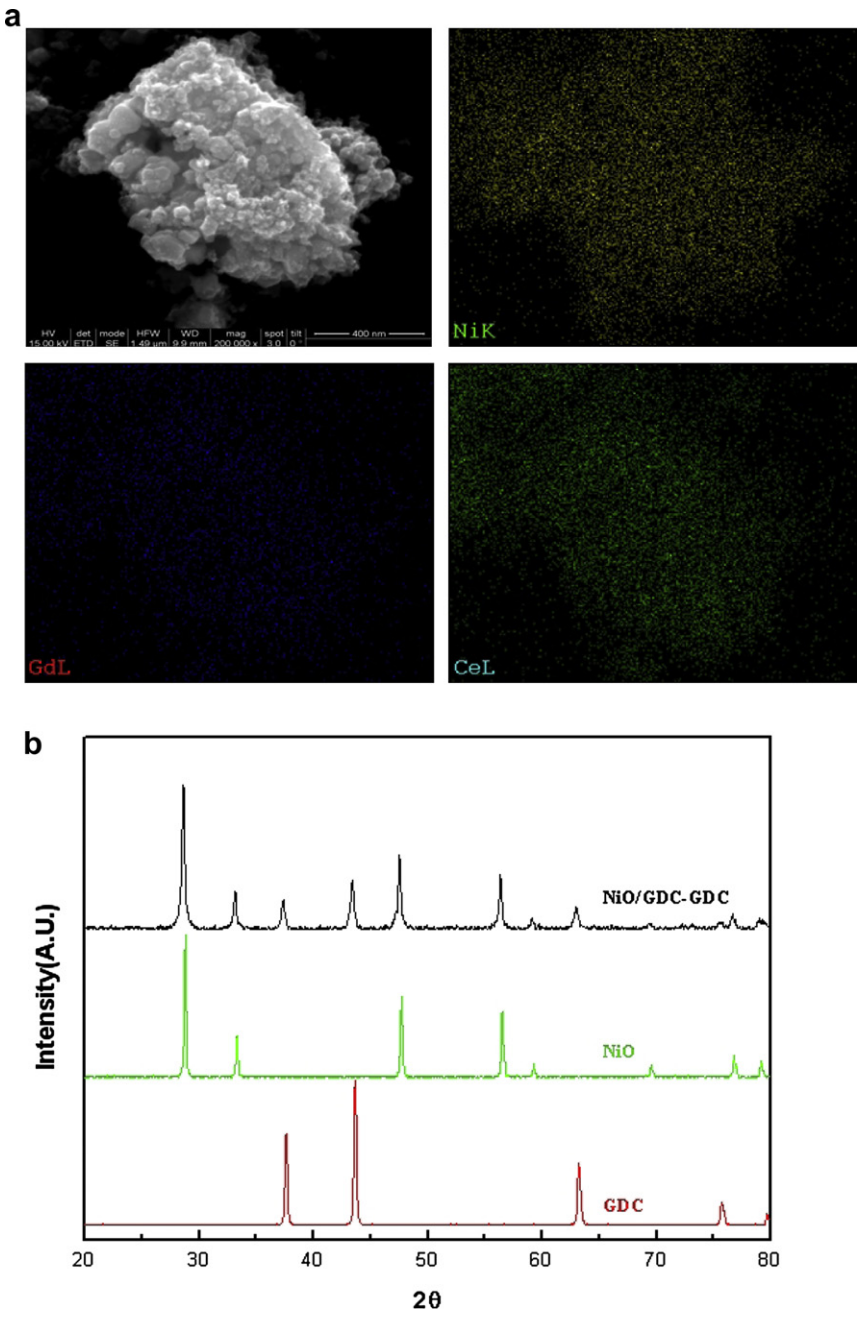

Fig. 3 – (a) SEM-EDX images and (b) XRD data of the NiO/GDC–GDC nano-composite powder.

maintained its thermal stability over the 30 cycles of the thermal cycling test, whereas the stability of the NiO–GDC mechanical mixture anode drastically decreased after 15 cycles, as shown in Fig. 4. This ideal structure of the NiO/GDC–GDC powder enhances the sensitivity for these reactions due to the enlarged surface volume area with adhered NiO and GDC on the GDC. This was confirmed by the methane flow test in which the weight change due to deposited carbon on NiO–GDC and NiO/GDC–GDC powders in a methane atmosphere at 650 °C was monitored. As shown in Fig. 5, the weight of the NiO/GDC–GDC powder increased 512 wt%, which was 73 times more than the NiO–GDC powder, which increased 7 wt%. This is because the enlarged Ni surface area enhanced the methane cracking reaction (2). However, NiO/GDC–GDC not only led to an enhanced methane cracking reaction, but also prevented carbon deposition on the operating unit cell as adhered GDC on the core GDC acts as the catalyst on the three phase boundary for the electrochemical reaction (1) with dry methane and simultaneously oxidizes deposited carbon (3) by the methane cracking reaction (2) on the Ni catalyst.

$$CH_4 + 4O^{2-} \rightarrow CO_2 + 2H_2O + 8e^- \quad (1)$$

$$CH_4 \rightarrow C + 2H_2 \quad (2)$$

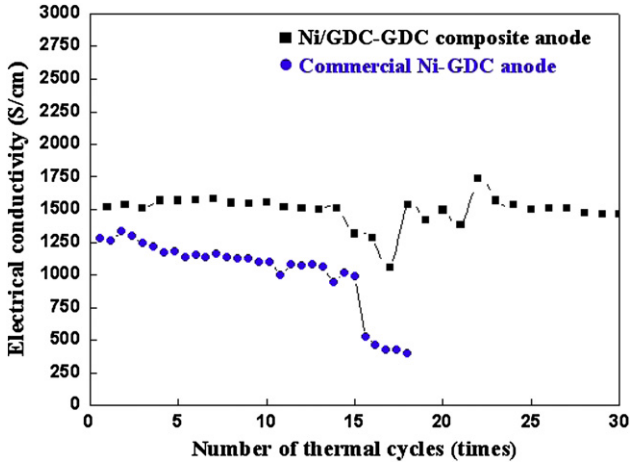

Fig. 4 – Thermal cycling stabilities of the NiO–GDC and NiO/GDC–GDC anodes.

$$C_{(s)} + 2O^{2-} \rightarrow CO_2 + 4e^- \quad (3)$$

It also increases the mechanical strength of the anode and the connectivity between the anode and electrolyte via sintering between the nano-sized GDC and core GDC. In our previous report, the advantages of dual nano-composite powders were discussed in more detail for SOFC anodes.

3.2. *Optimization of the tape-casting/lamination/co-firing technique*

The flatness of planar SOFCs strongly influences the cell performance because a flatter cell increases the contact area of the current collectors and reduces the possibility of cracking or fracturing of the unit cell. In our previous reports, we determined that the key contributors for the flatness of planar SOFCs are the heat treatment schedule and applying load during co-firing as well as the flatness of each green sheet [25]. The anode-supported electrolyte was fabricated via co-firing laminations of green sheets of anode and electrolyte. In order to improve the flatness of the laminate, the viscosity of the anode slurry was increased to cast a 100-μm anode sheet. Also, the thickness ratio of the anode and electrolyte was optimized to obtain a higher cell performance with minimized ohmic resistance. As a result of reducing the thickness of the electrolyte sheet from 28 μm to 18 μm, the flatness of the co-fired laminate increased from 89 μm/5 cm to 116 μm/5 cm and the performance also improved from 4.3 W to 6.1 W, as shown in Fig. 6. Although the thickness of the electrolyte can be minimized to 5 μm by tape-casting in our laboratory, the electrolyte was casted at 18 μm to maintain the mechanical/chemical stability in a reduction atmosphere with a large enough open circuit voltage. Finally, the thickness of the anode green sheet was increased from 25 μm to 100 μm by controlling the slurry viscosity, as we previously reported. This co-fired laminate had a flatness of 55 μm/5 cm and a cell performance of 6.3 W, which represents a 25% improvement compared to the previous cells.

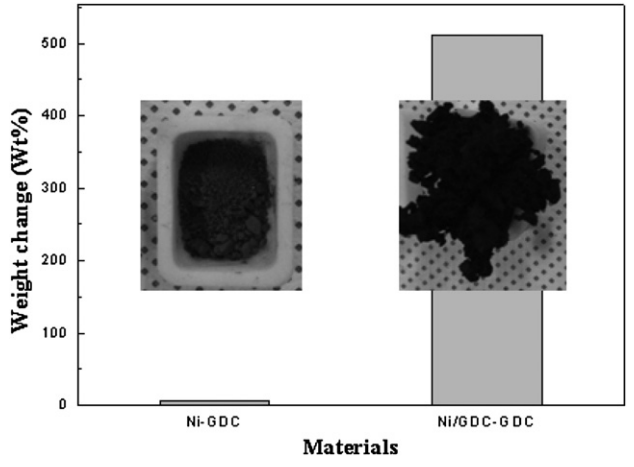

Fig. 5 – Weight changes and digital images of the methane flow test results for the NiO–GDC and NiO/GDC–GDC anodes.

3.3. *Cell performance evaluation*

4 types of unit cells were prepared after securing the flatness of lamination at about 50–60 μm/5 cm and cutting as a button-type unit cell. The most conventional cell 1 was fabricated from a laminate of a NiO–GDC anode and GDC electrolyte and co-fired at 1400 °C while the LSCF–GDC cathode was formed via screen-printed and additory firing at 1000 °C. In cell 2 and cell 3, an anode functional layer containing a mechanical mixture of NiO–GDC and NiO/GDC–GDC dual nano-composite powder was inserted to reduce the electrode resistance and interfacial resistance between the anode and electrolyte as well as to enlarge the three-phase boundary. The anodes of cell 4 only consisted of NiO/GDC–GDC dual nano-composite powder. The power density of cell 1 was 0.4 W/cm^2 with H_2 and 0.3 W/cm^2 with CH_4 at 650 °C. As shown in Fig. 7, the NiO–GDC functional layer of cell 2 slightly affected the electrode and interfacial resistances, which decreased from 0.23 Ω cm^2 to 0.18 Ω cm^2 and from 0.18 Ω cm^2 to 0.15 Ω cm^2, respectively. However, the conventional NiO–GDC AFL has a low porosity and surface area, which had results in the decline of three phase boundary and cell performances. The rapid decrease in cell performances was occurred during the direct electrochemical reaction with dry methane that used a GDC catalyst due to less GDC surface area. However, in the case of the NiO/GDC–GDC AFL, it significantly affected the electrode and interfacial resistances because, which were 0.11 Ω cm^2 and 0.13 Ω cm^2, respectively. From the comparison of the ASR data of cell 1, cell 2, and cell 3, it was demonstrated that the anode functional layers provide better connectivity between the anode and electrolyte through reduced interfacial resistance. Nonetheless, when the AFL consisted of the same raw materials as the anode, it did not affect the electrode resistance as much as in the case of NiO/GDC–GDC. Cell 4 used NiO/GDC–GDC dual nano-composite powder as the anode support, which considerably

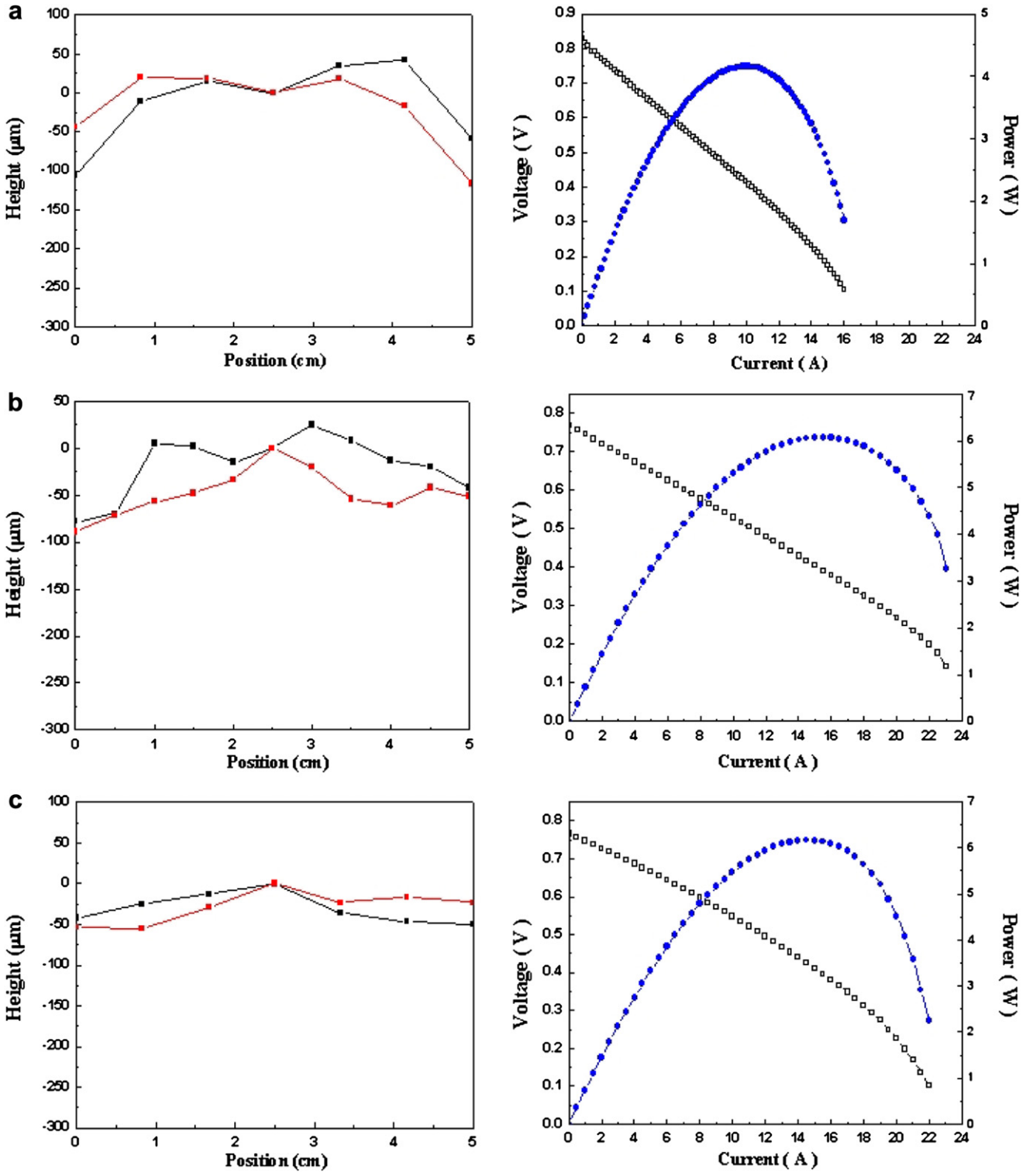

Fig. 6 – Flatness and cell performances of unit cells fabricated with (a) a 28 μm electrolyte and 25 μm anode green sheets, (b) a 18 μm electrolyte and 25 μm anode green sheets, and (c) a 18 μm electrolyte and 100 μm anode green sheets after sintering with a loading of 11.3 g/cm^2.

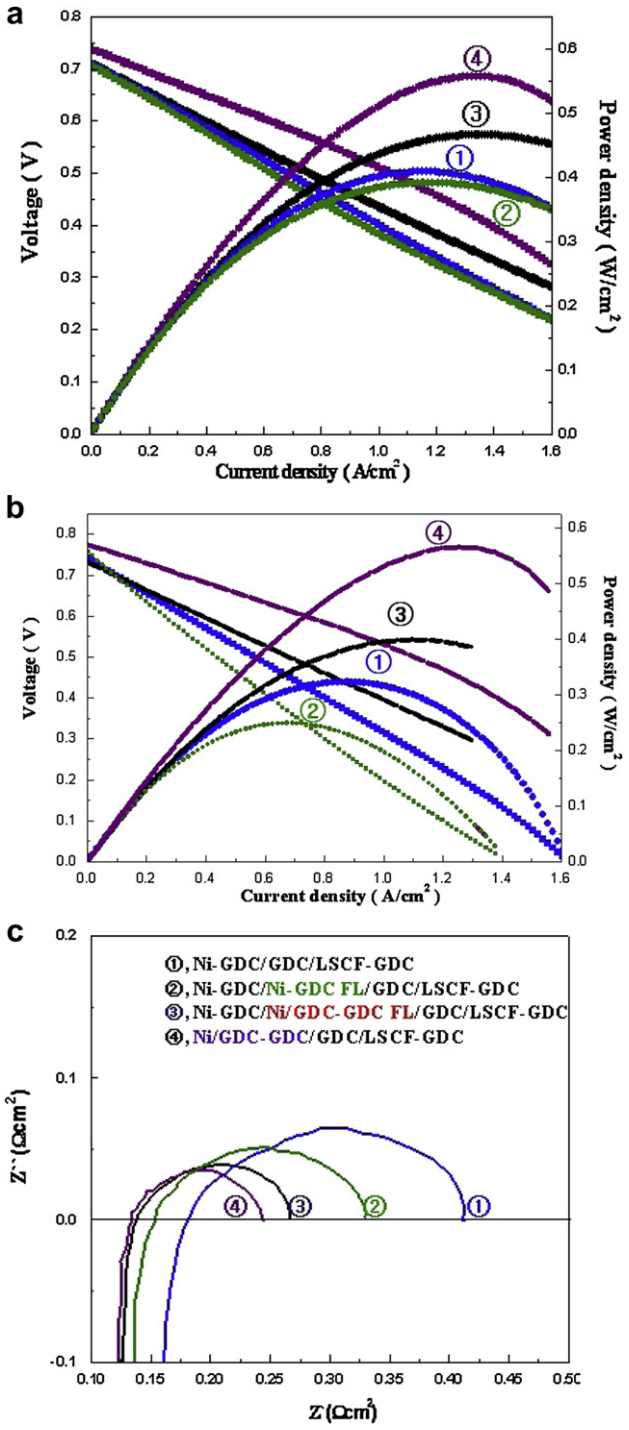

Fig. 7 – Cell performances with (a) H_2 and (b) CH_4 as well as (c) ASR data of cell 1 (①), cell 2 (②), cell 3 (③), and cell 4 (④) at 650 °C.

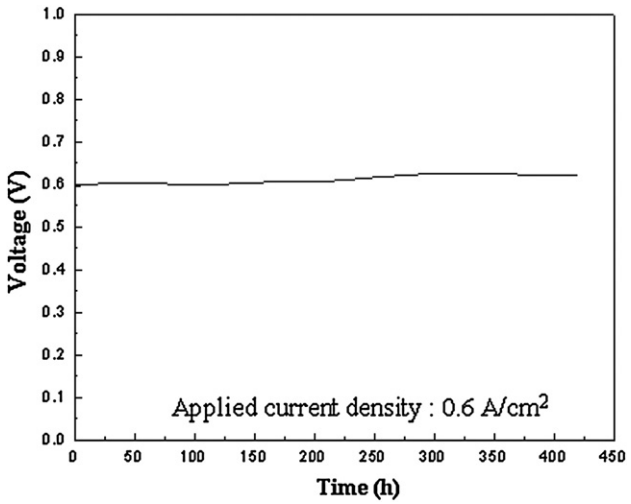

Fig. 8 – Long-term stability test results of cell 4 with CH_4 at 650 °C.

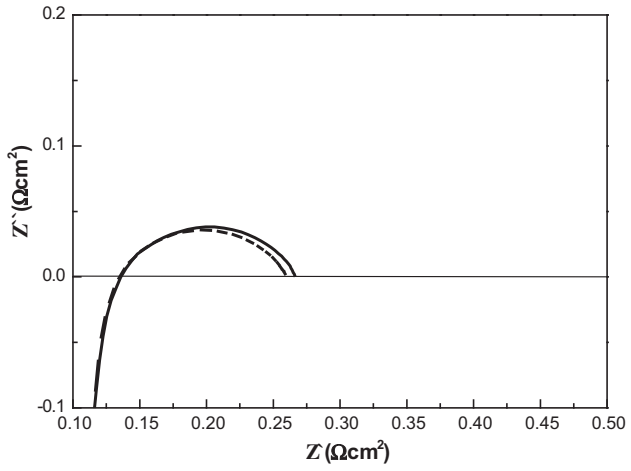

Fig. 9 – Impedance spectra of cell 4 (—) before and (---) after long-term stability test with methane.

improved the power density to 0.56 W/cm^2 with H_2 and CH_4 due to the minimal electrode and interfacial resistances. In addition, NiO/GDC–GDC facilitated the long-term stability tests as the adhered GDC nano-particles oxidized deposited carbon. As shown in Fig. 8, cell 4 could be stably operated for 500 h with dry methane without any degradation. The impedance spectra of the cell 4 before and after long-term stability test for 500 h with dry methane decreased the electrode resistance from 0.1303 Ω cm^2 to 0.1233 Ω cm^2, because the "carbon bridges" affected on connectivity between the nickel particles as shown in Fig. 9 [26]. This carbon did not continuously deposit on the nickel, only a certain amount of carbon was maintained by reaction (3) of deposited carbon with use of a large enough flux of O^{2-} ions through the GDC electrolyte [27,28]. Finally, cell 1 and cell 4 were enlarged as 5 × 5 cm^2 planar-type unit cells and these cells showed maximum powers of 6.3 W with H_2 and 5.5 W with CH_4, and 9.54 W with H_2 and 8.2 W with CH_4, respectively, as shown in Fig. 10.

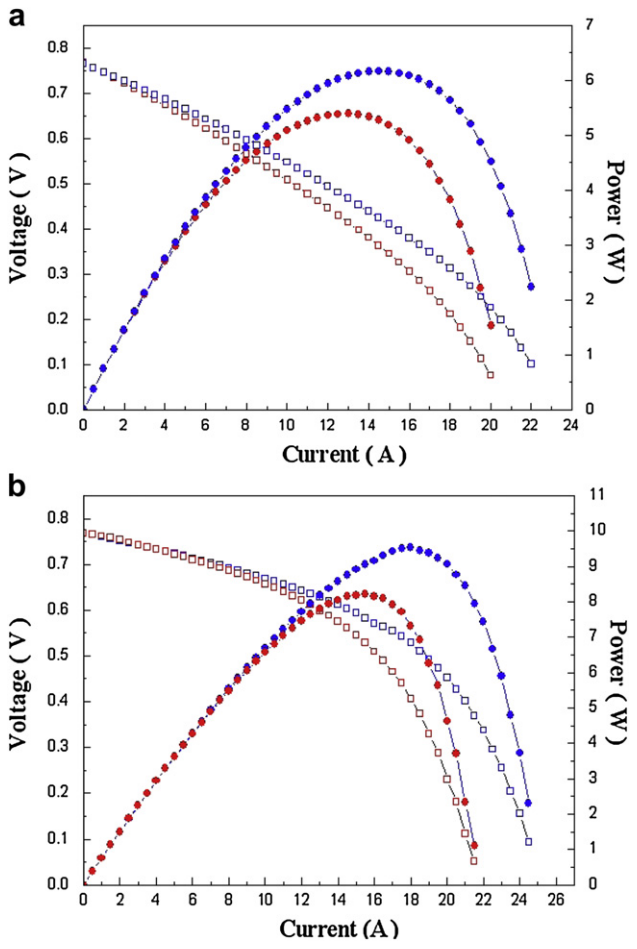

Fig. 10 – Cell performance of 5 × 5 cm^2 planar-type unit cells of (a) cell 1 and (b) cell 2 with H_2 and CH_4 at 650 °C.

4. Conclusion

The tape-casting/lamination/co-firing technique was used to fabricate cost-effective large-scale unit cells. The 55 μm/5 cm flatness unit cells could be obtained after optimization using 18 μm electrolyte and 100 μm thick anode green tapes. NiO/GDC–GDC nano-composite powder was synthesized by the Pechini process, which reduces the electrode resistance and interfacial resistance due to the better connectivity between the anode and electrolyte. Moreover, adhered NiO and GDC nano-particles on GDC resulted in improved cell performance with an enlarged three-phase boundary, prevented carbon cocking by oxidizing the deposited carbon, and enhanced the thermo-cyclic stability. For cell 1 and cell 4, it was confirmed that the NiO/GDC–GDC anode-supported unit cell improved the cell performance 50% more than the non-AFL unit cells. In addition, cell 4 could be operated for over 500 h without degradation. The large-scale 5 × 5 cm^2 NiO/GDC–GDC anode-supported unit cell showed maximum powers of 9.54 W and 8.2 W with hydrogen and dry methane, respectively.

Acknowledgments

This work was supported by the Seoul R&BD Program (CS070157).

REFERENCES

[1] Zhu WZ, Deevi SC. A review on the status of anode materials for solid oxide fuel cells. Materials Science and Engineering A 2003;362:228–39.
[2] Lee DS, Kim WS, Choi SH, Kim J, Lee HW, Lee JH. Characterization of ZrO_2 co-doped with Sc_2O_3 and CeO_2 electrolyte for the application of intermediate temperature SOFCs. Solid State Ionics 2005;176:33–9.
[3] Jung HY, Choi SH, Kim H, Son JW, Kim J, Lee HW, et al. Fabrication and performance evaluation of 3-cell SOFC stack based on planar 10 cm × 10 cm anode-supported cells. Journal of Power Sources 2006;159:478–83.
[4] Wen TL, Wang D, Tu HY, Chen M, Lu Z, Zhang Z, et al. Research on planar SOFC stack. Solid State Ionics 2002;152-153:399–404.
[5] Maček J, Novosel B, Marinšek M. Ni–YSZ SOFC anodes — Minimization of carbon deposition. Journal of the European Ceramic Society 2007;27:487–91.
[6] Nikooyeh K, Clemmer R, Alzate-Restrepo V, Hill JM. Effect of hydrogen on carbon formation on Ni/YSZ composites exposed to methane. Applied Catalysis A: General 2008;347:106–11.
[7] Laosiripojana N, Assabumrungrat S. Catalytic steam reforming of methane, methanol, and ethanol over Ni/YSZ: the possible use of these fuels in internal reforming SOFC. Journal of Power Sources 2007;163:943–51.
[8] Gorte RJ, Vohs JM, McIntosh S. Recent developments on anodes for direct fuel utilization in SOFC. Solid State Ionics 2004;175:1–6.
[9] Myung JH, Lee JJ, Hyun SH. Performance improvement of oxide catalyst-doped anode-supported SOFCs for methane fuel. Electrochemical and Solid-State Letters 2010;13:B43–5.
[10] Myung JH, Ko HJ, Lee JJ, Hyun SH. Optimization of flow rate for improving performance and stability of NI-YSZ based solid oxide fuel cells using CH_4 fuel. International Journal of Electrochemical Science 2011;6:1617–29.
[11] Huang K, Goodenough JB. A solid oxide fuel cell based on Sr- and Mg-doped $LaGaO_3$ electrolyte: the role of a rare-earth oxide buffer. Journal of Alloys and Compounds 2000;303–304:454–64.
[12] Huang K, Wan JH, Goodenough JB. Increasing power density of LSGM-based solid oxide fuel cells using new anode materials. Journal of the Electrochemical Society 2001;148:A788–94.
[13] Yan J, Matsumoto H, Enoki M, Ishihara T. High-power SOFC using $La_{0.9}Sr_{0.1}Ga_{0.8}Mg_{0.2}O_3$-δ/$Ce_{0.8}Sm_{0.2}O_2$-δ composite film. Electrochemical and Solid-State Letters 2005;8:A389–91.
[14] Costa-Nunes O, Gorte RJ, Vohs JM. Comparison of the performance of Cu–CeO_2–YSZ and Ni–YSZ composite SOFC anodes with H_2, CO, and syngas. Journal of Power Sources 2005;141:241–9.
[15] Gorte RJ, Kim H, Vohs JM. Novel SOFC anodes for the direct electrochemical oxidation of hydrocarbon. Journal of Power Sources 2002;106:10–5.
[16] Lu C, Worrell WL, Wang C, Park S, Kim H, Vohs JM, et al. Development of solid oxide fuel cells for the direct oxidation of hydrocarbon fuels. Solid State Ionics 2002;152–153:393–7.
[17] Lee JJ, Park EW, Hyun SH. Performance and evaluation of Cu-based nano-composite anodes for direct utilisation of hydrocarbon fuels in SOFCs. Fuel Cells 2010;10:145–55.
[18] Kim S-D, Moon H, Hyun S-H, Moon J, Kim J, Lee H-W. Ni-YSZ cermet anode fabricated from NiO-YSZ composite powder for high-performance and durability of solid oxide fuel cells. Solid State Ionics 2007;178:1304–9.
[19] Kim S-D, Moon H, Hyun S-H, Moon J, Kim J, Lee H-W. Nano-composite materials for high-performance and durability of

solid oxide fuel cells. Journal of Power Sources 2006;163:392–7.
[20] Kim S-D, Moon H, Hyun S-H, Moon J, Kim J, Lee H-W. Performance and durability of Ni-coated YSZ anodes for intermediate temperature solid oxide fuel cells. Solid State Ionics 2006;177:931–8.
[21] Myung J-H, Ko HJ, Park H-G, Hwan M, Hyun S-H. Fabrication and characterization of planar-type SOFC unit cells using the tape-casting/lamination/co-firing method. International Journal of Hydrogen Energy 2012;37:498–504.
[22] Moon H, Kim SD, Park EW, Hyun SH, Kim HS. Characteristics of SOFC single cells with anode active layer via tape casting and co-firing. International Journal of Hydrogen Energy 2008;33:2826–33.
[23] Moon H, Kim SD, Hyun SH, Kim HS. Development of IT-SOFC unit cells with anode-supported thin electrolytes via tape casting and co-firing. International Journal of Hydrogen Energy 2008;33:1758–68.
[24] Park H-G, Moon H, Park S-C, Lee J-J, Yoon D, Hyun S-H, et al. Performance improvement of anode-supported electrolytes for planar solid oxide fuel cells via a tape-casting/lamination/co-firing technique. Journal of Power Sources 2010;195:2463–9.
[25] Moon H, Kang D-W, Park H-G, Hyun S-H. Stress and camber analysis of anode-supported electrolytes by tape-casting and co-firing techniques. International Journal of Hydrogen Energy 2011;36:10991–7.
[26] McIntosh S, Vohs JM, Gorte RJ. Role of hydrocarbon deposits in the enhanced performance of direct-oxidation SOFCs. Journal of the Electrochemical Society 2003;150:A470–6.
[27] Liu J, Barnett SA. Operation of anode-supported solid oxide fuel cells on methane and natural gas. Solid State Ionics 2003;158:11–6.
[28] Dhir A, Kendall K. Microtubular SOFC anode optimisation for direct use on methane. Journal of Power Sources 2008;181:297–303.